Optimization of synchronization in complex clustered networks

Liang Huang
Department of Electrical Engineering, Arizona State University, Tempe, Arizona 85287, USA

Ying-Cheng Lai
Department of Electrical Engineering and Department of Physics and Astronomy, Arizona State University, Tempe, Arizona 85287, USA

Robert A. Gatenby
Department of Radiology and Department of Applied Mathematics, University of Arizona, Tucson, Arizona 85721, USA

(Received 7 August 2007; accepted 28 November 2007; published online 8 January 2008)

There has been mounting evidence that many types of biological or technological networks possess a clustered structure. As many system functions depend on synchronization, it is important to investigate the synchronizability of complex clustered networks. Here we focus on one fundamental question: Under what condition can the network synchronizability be optimized? In particular, since the two basic parameters characterizing a complex clustered network are the probabilities of intercluster and intracluster connections, we investigate, in the corresponding two-dimensional parameter plane, regions where the network can be best synchronized. Our study yields a quite surprising finding: a complex clustered network is most synchronizable when the two probabilities match each other approximately. Mismatch, for instance caused by an overwhelming increase in the number of intracluster links, can counterintuitively suppress or even destroy synchronization, even though such an increase tends to reduce the average network distance. This phenomenon provides possible principles for optimal synchronization on complex clustered networks. We provide extensive numerical evidence and an analytic theory to establish the generality of this phenomenon. © *2008 American Institute of Physics*. [DOI: 10.1063/1.2826289]

The complex-network approach has recently been used widely to investigate and understand the dynamics and statistical properties of many-body systems, such as neuron systems[1] and computer networks.[2,3] Synchronization is one of the fundamental properties characterizing the collective motion of a complex many-body system. There has been much interest in this topic, but most existing works have focused on the small-world[4] and the scale-free[5] network topologies. In the past several years, the importance of complex clustered topology has been recognized, especially in biological, social, and certain technological networks. Such a network can be represented by a collection of sparsely linked clusters of nodes, where the connectivity within any individual cluster is dense. Examples of complex clustered networks include certain computer networks,[2,3] protein-protein interaction networks,[6–8] and metabolic graphs.[9] Investigation of synchronization in complex clustered networks has begun only recently.[10,11] In this paper we focus on one basic question: under what condition can the synchronizability of a complex clustered network be optimized? One way to address this question is to recognize the two basic parameters characterizing a complex clustered network: the probabilities of intercluster and intracluster connections. It is thus insightful to investigate, in the corresponding two-dimensional parameter plane, regions where the network can be best synchronized. Our study yields a quite surprising finding: a complex clustered network is most synchronizable when the two probabilities match each other approximately. Mismatch, for instance caused by an overwhelming increase in the number of intracluster links, can counterintuitively suppress or even destroy synchronization, even though such an increase tends to reduce the average network distance. This suggests that, to achieve robust synchronization in a complex clustered network, simply counting the number of links is not enough. Instead, links should be classified carefully and placed properly between or within the clusters to optimize possible synchronization-related functions of the network. The potential significance of our result can be illustrated by a specific example: efficient computation on a computer network. Suppose a large-scale, parallel computational task is to be accomplished by the network, for which synchronous timing is of paramount importance. Our result can provide useful clues as to how to design the network to achieve the best possible synchronization and consequently optimal computational efficiency.

I. INTRODUCTION

Recent years have witnessed a growing interest in the synchronizability of complex networks.[12–24] Earlier works[12–18] suggest that small-world[4] and scale-free[5] networks, due to their small network distances, are generally more synchronizable than regular networks. It has been found, however, that heterogeneous degree distributions typically seen in scale-free networks can inhibit their synchronizability,[19] but adding suitable weights to the net-

work elements can enhance their chances to synchronize with each other.[20–23] Synchronizability of complex clustered networks has begun to be studied only recently.[10,11] In particular, the dependence of synchronizability on the number of clusters in the network has been investigated in Ref. 10, with the result that a network can become more synchronizable with the number of clusters if there are random, long-range links. In the absence of such links, the synchronizability would deteriorate continuously as more clusters appear in the network.

Viewing biological cells in terms of their underlying network structure is a useful concept and has attracted much attention recently.[25–29] Over the past several years, network science has been developed and mathematical treatments have been employed to understand the relation between the topological structure of networks and their functions.[29–33] Organizing biological information using the network idea has been fundamental to utilizing various system-level approaches to understanding biological function. A key organizational feature in many biological systems is the tendency to form a clustered network structure.[6–9] For example, proteins with a common function are usually physically associated via stable protein-protein interactions to form larger macromolecular assemblies. These protein complexes (or clusters) are often linked together by extended networks of weaker, transient protein-protein interactions to form interaction networks that integrate pathways mediating the major cellular processes.[6,7] As a result, a protein-protein interaction network can be viewed naturally as an assembly of interconnected functional clusters, or a complex clustered network. Another example is the metabolic network of organisms. It has been found that various metabolic networks are organized into many small, highly connected clusters that combine in a hierarchical manner into larger, less cohesive units. For example, within the *Escherichia coli*, the uncovered hierarchical modularity is highly correlated with known metabolic functions. It is possible that the clustered network architecture is generic to system-level cellular organization.[9] Recent works have also revealed that the clustered topology is fundamental to many types of social and technological networks.[34–36]

In biology, synchronization is one of the most fundamental dynamics.[37] For examples, fireflies in Southeast Asia, stretching for miles along the river bank, by adjusting the rhythms on receiving signals from others, can flash synchronously.[38] The heart's pacemaker, the so-called sinoatrial node, consists of about 10 000 synchronous cells, and generates the electrical rhythm that commands the rest of the heart to beat.[39] Other examples include the rhythmic activity of cells of the pancreas[40] and of neural networks.[41] As the complex, clustered network topology is necessary for describing and understanding the dynamics and function of some key biological systems, it is important to study the synchronizability of such networks.

Given a complex network with a fixed (large) number of nodes, it is believed that its synchronizability can be improved by increasing the number of links. This is intuitive as a denser linkage makes the network more tightly coupled or, "smaller," thereby facilitating synchronization. However, we have recently published a short Letter[11] presenting a phenomenon that apparently contradicts this intuition. In particular, a complex clustered network is typically small-world, so that its average distance is small. Moreover, its degree distribution can be made quite homogeneous. The surprising phenomenon is that more edges (links), which make the network smaller, do not necessarily lead to stronger synchronizability. There can be situations where more edges can even suppress synchronization if they are placed improperly. We find that the synchronizability of a clustered network is largely determined by the interplay between the intercluster and the intracluster connections of the network. Strong synchronizability requires that the numbers of the interlinks and intralinks be approximately matched. In this case, increasing the number of links can indeed enhance the synchronizability. However, if the number of one type of links is fixed while the number of the other type is changed so that the matching is deteriorated, synchronization can be severely suppressed or even totally destroyed.

The oscillator models employed in our short Letter[11] are discrete-time maps. In biological and technological systems, however, continuous-time oscillator models are more realistic. One aim of this contribution is to address whether synchronization can be optimized in continuous-time oscillator networks with a clustered structure. Another aim is to generalize our finding by considering an alternative coupling scheme that has not been treated previously. We shall develop a theory based on analyzing the spectral properties of the network coupling matrix, which are the key to the network's ability to synchronize. Direct numerical simulations of a class of actual oscillator clustered networks provide strong support for the theory. From the viewpoint of computation, most previous works on network synchronization[12–24] are focused on the eigenvalue properties of the underlying networks. The numerical results in this paper are from *direct assessment* of whether or not the underlying oscillator network can achieve synchronization, which involves quite intense computations. Our results imply that, in order to achieve robust synchronization for a clustered biological or technological network, the characteristics of the links are more important than the number of links. Simply counting the number of links may not be enough to determine its synchronizability. Instead, links should be carefully distinguished and classified to predict possible synchronization-related functions of the network.

In Sec. II, we describe a general linear-stability analysis for dealing with synchronization in continuous-time oscillator networks. In Sec. III, we develop theory and present numerical results for optimization of synchronization in complex clustered networks. To be as general as possible, two types of coupling schemes have been considered. An extensive discussion of the main result and its biological implications is offered in Sec. IV.

II. LINEAR-STABILITY ANALYSIS FOR SYNCHRONIZATION IN CONTINUOUS-TIME OSCILLATOR NETWORKS

The approach we take to establish the result is to introduce nonlinear dynamics on each node in the network and

then perform stability and eigenvalue analyses.[42,43] The theoretical derivation yields the stability regions for synchronization in the two-dimensional parameter space defined by the probabilities of the two types of links. The analytic predictions are verified by direct numerical simulations of the dynamical network. To be specific, in this paper we consider the following general clustered network model: N nodes are classified into M groups, where each group has $n=N/M$ nodes. In a group, a pair of nodes is connected with probability p_s, and nodes belonging to different groups are connected with probability p_l. This forms a clustered random network. For a clustered network, the number of interconnections is typically far less than the number of intraconnections. As a result, the parameter region of small p_l values is more relevant.

We consider the synchronization condition of clustered networks of continuous-time oscillators in the network parameter space. Each oscillator, when isolated, is described by

$$\frac{d\mathbf{x}}{dt} = \mathbf{F}(\mathbf{x}), \tag{1}$$

where $\mathbf{x}$ is a d-dimensional vector and $\mathbf{F}(\mathbf{x})$ is the velocity field. Without loss of generality we choose a prototype oscillator model—the Rössler oscillator—for which $\mathbf{x}=[x,y,z]^T$ ($[*]^T$ denotes transpose), and

$$\mathbf{F}(\mathbf{x}) = [-(y+z), x+0.2y, 0.2+z(x-9)]^T. \tag{2}$$

The parameters of the Rössler oscillator are chosen such that it oscillates chaotically. The network dynamics are described by

$$\frac{d\mathbf{x}_i}{dt} = \mathbf{F}(\mathbf{x}_i) - \epsilon\sum_{j=1}^{N} G_{ij}\mathbf{H}(\mathbf{x}_j), \tag{3}$$

where $\mathbf{H}(\mathbf{x})=[x,0,0]^T$ is a linear coupling function, ϵ is global coupling parameter, and $\mathbf{G}$ is the coupling matrix describing the network topology (to be explained below). The matrix $\mathbf{G}$ satisfies the condition $\Sigma_{j=1}^{N} G_{ij}=0$ for any i, where N is the network size, therefore the system permits an exact synchronized solution: $\mathbf{x}^1=\mathbf{x}^2=\cdots=\mathbf{x}^N=\mathbf{s}$, where $d\mathbf{s}/dt=\mathbf{F}(\mathbf{s})$. Since the couplings can be weighted, we will consider two typical types of coupling schemes (to be explained below).

For the system described by Eq. (3), the variational equations governing the time evolution of the set of infinitesimal vectors $\delta\mathbf{x}_i(t)\equiv\mathbf{x}_i(t)-\mathbf{s}(t)$ are

$$\frac{d\delta\mathbf{x}_i}{dt} = \mathbf{DF}(\mathbf{s})\cdot\delta\mathbf{x}_i - \epsilon\sum_{j=1}^{N} G_{ij}\mathbf{DH}(\mathbf{s})\cdot\delta\mathbf{x}_j, \tag{4}$$

where $\mathbf{DF}(\mathbf{s})$ and $\mathbf{DH}(\mathbf{s})$ are the Jacobian matrices of the corresponding vector functions evaluated at $\mathbf{s}(t)$. Diagonalizing the coupling matrix G yields a set of eigenvalues $\{\lambda_i, i=1,\ldots,N\}$ and the corresponding normalized eigenvectors are denoted by $\mathbf{e}_1,\mathbf{e}_2,\ldots,\mathbf{e}_N$. The eigenvalues are real and non-negative and can be sorted as $0=\lambda_1<\lambda_2\leq\cdots\leq\lambda_N$.[43] The smaller the ratio λ_N/λ_2, the stronger the synchronizability of the network.[19–23] The transform $\delta\mathbf{y}=O^{-1}\cdot\delta\mathbf{x}$, where O is a matrix whose columns are the set of eigenvectors, leads to the block-diagonally decoupled form of Eq. (4):

$$\frac{d\delta\mathbf{y}_i}{dt} = [\mathbf{DF}(\mathbf{s}) - \epsilon\lambda_i\mathbf{DH}(\mathbf{s})]\cdot\delta\mathbf{y}_i.$$

Letting $K=\epsilon\lambda_i$ $(i=2,\ldots,N)$ be the normalized coupling parameter, we can write

$$\frac{d\delta\mathbf{y}}{dt} = [\mathbf{DF}(\mathbf{s}) - K\mathbf{DH}(\mathbf{s})]\cdot\delta\mathbf{y}. \tag{5}$$

The largest Lyapunov exponent from Eq. (5) is the master-stability function $\Psi(K)$.[42] If $\Psi(K)$ is negative, a small disturbance from the synchronization state will diminish exponentially; thus, the system is stable and can be synchronized; if $\Psi(K)$ is positive, a small disturbance will be magnified and the system cannot be synchronized.

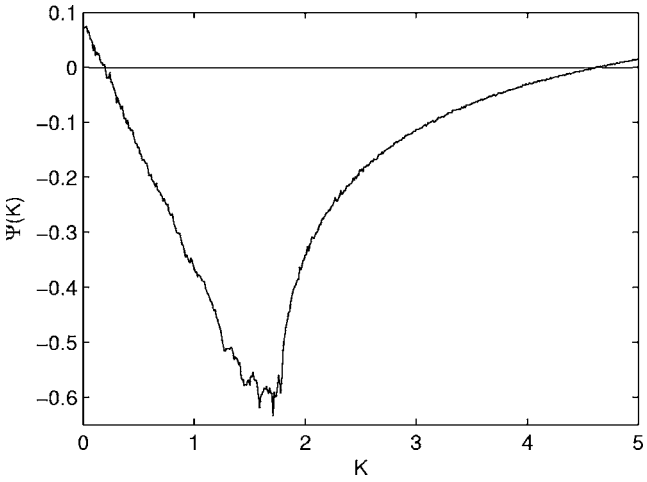

FIG. 1. For the Rössler oscillator network, an example of the master stability function $\Psi(K)$ calculated numerically from Eq. (5).

For the Rössler oscillators we used in the simulation, an example of the master stability function is shown in Fig. 1. The function $\Psi(K)$ is negative in the interval $[K_1,K_2]$, where $K_1\approx 0.2$ and $K_2\approx 4.62$. Thus, for $K_1<K<K_2$, all eigenvectors (eigenmodes) are transversely stable and the network can be synchronized, which gives the condition of the boundary of synchronization region:

$$\lambda_2 \geq \frac{K_1}{\epsilon}, \tag{6}$$

$$\lambda_N \leq \frac{K_2}{\epsilon}. \tag{7}$$

The boundaries determined by these equations and the numerical simulation results are shown in Fig. 2 for type-I coupling and Fig. 7 for type-II coupling. The analysis and the numerical result agree well.

III. SYNCHRONIZATION IN CONTINUOUS-TIME OSCILLATOR CLUSTERED NETWORKS

We shall consider two types of distinct coupling schemes for complex clustered networks and develop theoretical analysis for synchronization.

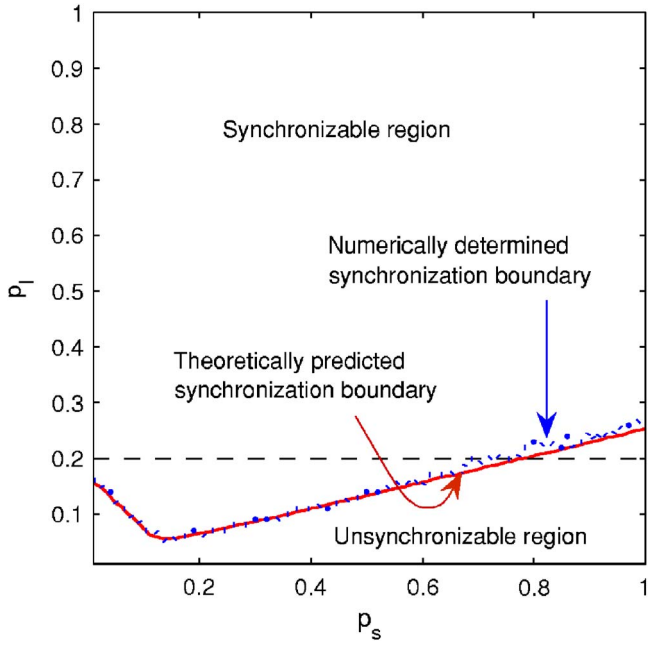

FIG. 2. (Color online) Synchronization boundary of the coupled Rössler oscillators on a two-cluster network. The dotted line is the numerically obtained boundary from the computation of $P_{\rm syn}$; the solid line is from theoretical analysis [Eq. (6)], where λ_2 is calculated numerically. The horizontal dashed line indicates the position of the cross section of $P_{\rm syn}$ shown in Fig. 3. Simulation parameters are $N=100$, $M=2$, $\delta=0.01$, $T_0=10^4$, and $\epsilon=0.5$. Each datapoint is the result of averaging over 1000 network realizations. The data for this figure was obtained with five Pentium®-IV 2.80 GHz CPUs for about two weeks.

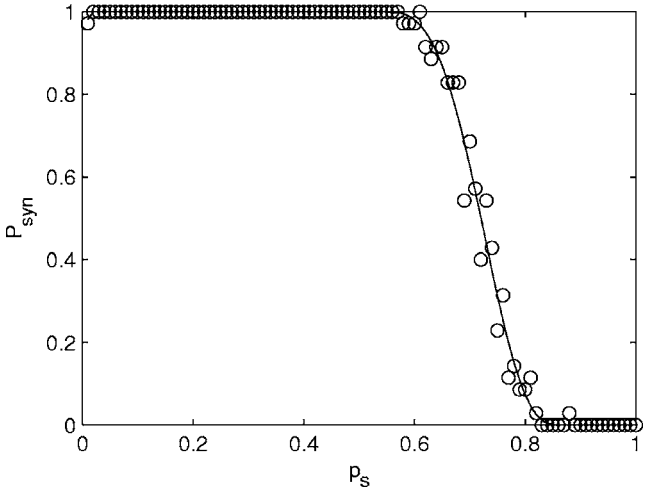

FIG. 3. Synchronization probability $P_{\rm syn}$ vs p_s for $p_l=0.2$ of a clustered network of Rössler oscillators with $N=100$ and $M=2$. $\delta=0.01$, $T_0=10^4$, and $\epsilon=0.5$. Each datapoint is the result of averaging over 1000 network realizations.

A. Type-I coupling

For type-I coupling, we consider a normalized coupling matrix: for any i $(1\leqslant i\leqslant N)$, $G_{ii}=1$, $G_{ij}=-1/k_i$ if there is a link between nodes i and j, and $G_{ij}=0$ otherwise, where k_i is the degree of node i (the number of links). The coupling matrix $\mathbf{G}$ is not symmetric since $G_{ij}=-1/k_i$, while $G_{ji}=-1/k_j$. Depending on the initial conditions and the network realization, the Rössler system may have desynchronization bursts.[44,45] It is thus necessary to characterize the network synchronizability in a statistical way. Define $P_{\rm syn}$ as the probability that the fluctuation width of the system $W(t)$ is smaller than a small number δ (chosen somewhat arbitrarily) at all time steps during a long observational period T_0 in the steady state, say, from T_1 to T_1+T_0, where $W(t)=\langle|x(t)-\langle x(t)\rangle|\rangle$, and $\langle\cdot\rangle$ means average over the nodes of the network. If δ is small enough, the system can be deemed as being synchronized in the period T_0; thus, $P_{\rm syn}$ is in fact the probability of synchronization of the system in the period T_0, with $P_{\rm syn}=1$ if the networks for the given parameters can synchronize. Practically, $P_{\rm syn}$ can be calculated by the ensemble average; i.e., the ratio of the number of synchronized cases over the number of all random network realizations. In addition, the ensemble average and time average of fluctuation width $\langle\langle W\rangle_{T_0}\rangle_e$ can be a direct indicator of the degree of synchronization, too. Since $P_{\rm syn}$ changes drastically from 0 to 1 in a small region in the parameter space, it is possible to define the boundary between synchronizable region and unsynchronizable region as follows: for a fixed p_s, the boundary value p_{lb} is such that the quantity $\|\nabla P_{\rm syn}(p_s,p_l)\|\equiv\sqrt{(\partial P_{\rm syn}/\partial p_s)^2+(\partial P_{\rm syn}/\partial p_l)^2}|_{(p_s,p_l)}$ is maximized at (p_s,p_{lb}). Figure 2 shows the synchronization boundary in the parameter space (p_s,p_l) from both numerical calculation and theoretical prediction of Eqs. (6) and (7). It can be seen that the two results agree with each other. If the number of intercluster connections is fixed, say, $p_l=0.2$ (the dashed line in Fig. 2), as the number of intracluster links exceeds a certain value (as p_s exceeds 0.78), the system becomes desynchronized. Figure 3 shows the synchronization probability $P_{\rm syn}$ on the dashed line in Fig. 2. When p_s is small, e.g., around 0.2, the number of the intercluster connections and the number of the intracluster connections are approximately matched, and the networks are synchronized. As p_s becomes larger and larger, the matching condition deteriorates, the networks lose their synchronizability, even though their average distances become smaller. That is, too many intracluster links tend to destroy the global synchronization. The same phenomenon persists for different parameter values. One remark concerning the physical meaning of the result, as exemplified by Figs. 2 and 3, is in order. Consider two clustered networks where (A) the two types of links are approximately matched and (B) there is a substantial mismatch. Our theory would predict that network A is more synchronizable than network B. This statement is meaningful in a probabilistic sense, as whether or not a specific system may achieve synchronization is also determined by many other factors such as the choice of the initial condition, possible existence of multiple synchronized states, and noise, etc. Our result means that, under the influence of these random factors, there is a higher probability for network A to be synchronized than network B.

Figure 4 shows the dependence of λ_N and λ_2 on the network parameters (p_l, p_s) for the two-cluster network. The shape of the boundary in Fig. 2 depends on the coupling strength ϵ [Eqs. (6) and (7)] and on the contour lines of λ_2 and λ_N. For the clustered network of Rössler oscillators, Eq. (7) is always satisfied. Thus, λ_2 determines the synchronizability of the system. In the following, we shall derive a

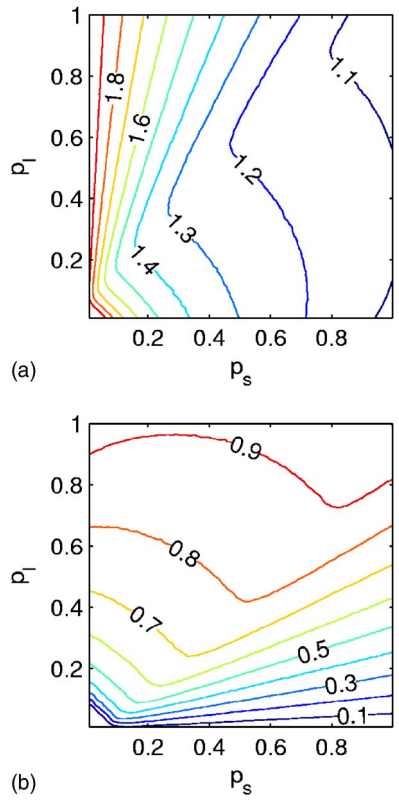

FIG. 4. (Color online) Contour plots of λ_N (a) and λ_2 (b) in the (p_l, p_s) space for type-I coupling. $N=100$ and $M=2$. Each datapoint is averaged over 100 realizations.

theoretical formula to understand the dependence of λ_2 on p_l and p_s for small values of p_l, which is the typical parameter regime of clustered networks.

For a clustered network, the components of the eigenvector $\mathbf{e}_2$ have approximately the same value within any cluster, while they can be quite different for different clusters, as demonstrated in Fig. 5. Thus, we can write $\mathbf{e}_2 \approx [\tilde{e}_1, \ldots, \tilde{e}_1, \tilde{e}_2, \ldots, \tilde{e}_2, \ldots, \tilde{e}_M, \ldots, \tilde{e}_M]^T$, and for each I, $1 \leqslant I \leqslant M$, there are n $\tilde{e}_I$'s in $\mathbf{e}_2$. By definition, $\mathbf{G}\cdot\mathbf{e}_2 = \lambda_2 \mathbf{e}_2$ and

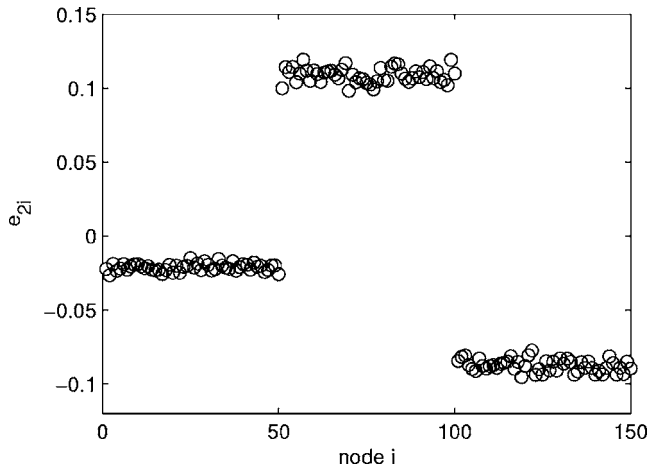

FIG. 5. A typical profile of components of the eigenvector $\mathbf{e}_2$. Parameters are $N=150$, $M=3$, $p_l=0.01$, and $p_s=0.9$.

$\mathbf{e}_2\cdot\mathbf{e}_2=1$, we have $\lambda_2=\mathbf{e}_2^T\cdot\mathbf{G}\cdot\mathbf{e}_2=\Sigma_{i,j=1}^N e_{2i}G_{ij}e_{2j}$, where e_{2i} is the ith component of $\mathbf{e}_2$. Expanding the summation in j yields

$$\lambda_2 = \sum_{i=1}^{N} e_{2i}\{G_{i1}\tilde{e}_1 + G_{i2}\tilde{e}_1 + \cdots + G_{in}\tilde{e}_1 + G_{in+1}\tilde{e}_2 + \cdots + G_{iN}\tilde{e}_M\}. \tag{8}$$

Recall that $G_{ii}=1$; and if i and j belong to the same cluster, G_{ij} equals $-1/k_i$ with probability p_s and 0 with probability $1-p_s$; while if i and j belong to different clusters, G_{ij} equals $-1/k_i$ with probability p_l and 0 with probability $1-p_l$, where k_i is the degree of node i. Thus,

$$\lambda_2 = \sum_{i=1}^{N} e_{2i}\left\{-n\frac{p_l}{k_i}\tilde{e}_1 - n\frac{p_l}{k_i}\tilde{e}_2 + \cdots + \tilde{e}_I - n\frac{p_s}{k_i}\tilde{e}_I + \cdots - n\frac{p_l}{k_i}\tilde{e}_M\right\},$$

where $\tilde{e}_I$ is the value corresponding to the cluster that contains node i. Noting that $1-np_s/k_i=(N-n)p_l/k_i$, we have

$$\lambda_2 = \sum_{i=1}^{N} e_{2i}\left\{(N-n)\frac{p_l}{k_i}\tilde{e}_I - n\frac{p_l}{k_i}\sum_{J\neq I}^{M}\tilde{e}_J\right\} = \sum_{i=1}^{N} e_{2i}\left\{N\frac{p_l}{k_i}\tilde{e}_I - n\frac{p_l}{k_i}\sum_{J=1}^{M}\tilde{e}_J\right\}.$$

For the clustered random network models, the degree distribution has a narrow peak centered at $k=np_s+(N-n)p_l$; thus, $k_i \approx k$. The summation over i can now be carried out in a similar manner,

$$\lambda_2 \approx \sum_{I=1}^{M} n\tilde{e}_I\left\{N\frac{p_l}{k}\tilde{e}_I - n\frac{p_l}{k}\sum_{J=1}^{M}\tilde{e}_J\right\} = N\frac{p_l}{k}\sum_{I=1}^{M} n\tilde{e}_I^2 - \left(n\sum_{J=1}^{M}\tilde{e}_J\right)^2\frac{p_l}{k}.$$

Note that $\Sigma_{I=1}^M n\tilde{e}_I^2 \approx \Sigma_{i=1}^N e_{2i}^2 = 1$, and $n\Sigma_{J=1}^M \tilde{e}_J = \Sigma_{i=1}^N e_{2i}$; thus, we have

$$\lambda_2 = \frac{Np_l}{np_s + (N-n)p_l} - \left(\sum_{i=1}^{N} e_{2i}\right)^2\frac{p_l}{k}. \tag{9}$$

The normalized eigenvector $\mathbf{e}_1$ of λ_1 corresponds to the synchronized state; thus, its components have constant values: $\mathbf{e}_1=[1/\sqrt{N}, \ldots, 1/\sqrt{N}]^T$. If $\mathbf{G}$ is symmetric, then eigenvectors for different eigenvalues are orthogonal; i.e., $\mathbf{e}_i\cdot\mathbf{e}_j=\delta_{ij}$, where $\delta_{ij}=1$ for $i=j$ and 0 otherwise. Taking $i=1$ and $j=2$, we have $\Sigma_{l=1}^N e_{2l}=0$. Although the coupling matrix $\mathbf{G}$ is slightly asymmetric, $\Sigma_{i=1}^N e_{2i}$ is nonzero but small, and the second term in Eq. (9) can be omitted, leading to the final form

$$\lambda_2 \approx \frac{Np_l}{np_s + (N-n)p_l}. \tag{10}$$

Since $n=N/M$, the above equation can be rewritten as

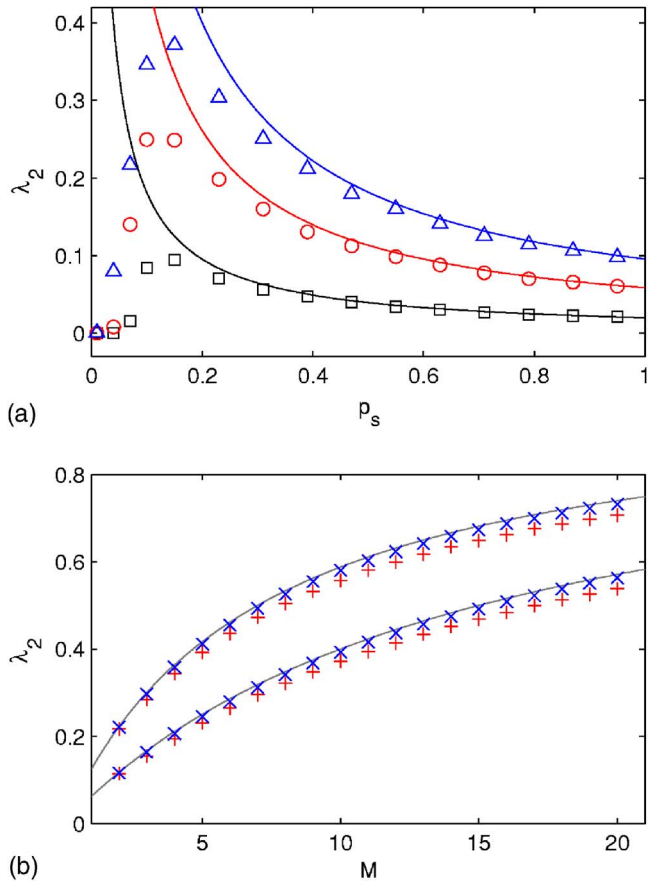

FIG. 6. (Color online) (a) λ_2 vs p_s for a network with two clusters. From bottom to top, p_l=0.01 (squares), p_l=0.03 (circles), and p_l=0.05 (up triangles). N=100 and n=50. (b) λ_2 vs the number of clusters M for n=50 (pluses) and n=200 (crosses). p_s=0.8; p_l=0.05 for the lower set of data and p_l=0.1 for the upper set of data. Note that the network size $N=Mn$ is changed with M. The symbols are obtained numerically and each data point is the average of 100 network realizations. The curves are from theory [Eq. (10)].

$$\lambda_2 \approx \frac{Mp_l}{p_s + (M-1)p_l}$$

or

$$\lambda_2 \approx \frac{Mp_l/p_s}{1 + (M-1)p_l/p_s}. \tag{11}$$

Figure 6(a) shows for several fixed p_l values, the dependence of λ_2 on p_s, from direct numerical calculation (symbols) and Eq. (10) (curves). For fixed p_l and large p_s, λ_2 decreases as p_s increases; thus, the network becomes more difficult to be synchronized. This provides an analytic explanation for the numerically observed abnormal behavior in the network synchronizability. For small p_s, when $p_s \sim p_l$, the network becomes a single random network; thus, λ_2 approximately follows the formula for random networks, which is an increasing function of p_s.[46] This makes clear the increasing behavior of λ_2 at small p_s cases. Furthermore, since λ_2 depends only on the ratio of p_l/p_s, this explains the straight-line patterns in Fig. 4(b) for $p_s > p_l$.

From Eq. (11), we can see that λ_2 is determined by the number of clusters M; it does not depend on the network size N, or the size of each cluster n, insofar as M is given. Figure 6(b) shows λ_2 versus M. The symbols are form direct numerical simulations and the curves are from theory [Eq. (11)] for two values of the ratio p_l/p_s: 0.05/0.8 and 0.1/0.8. Two cluster sizes (n=50 and n=200) are used. One can see that numerics agrees with the theory well for all cases. The larger cluster size case (crosses) agrees with the theory better. Since the synchronization boundaries is determined mainly by λ_2, it can be inferred that the synchronization boundary changes with the number of clusters. Even though the straight-line pattern of λ_2 in the (p_l, p_s) plane persists, thus the synchronization boundary in the plane will have a similar straight-line pattern as for the M=2 case, and our result that large p_s can deteriorate synchronization persists.

For large M values ($M \gg 1$), λ_2 can be approximated as $\lambda_2 \approx Mp_l/(p_s + Mp_l)$. For a given p_s value, the density of links within a cluster is fixed. Suppose the dynamical model of each node is also given; thus, the critical value of λ_2 for synchronization is fixed. As a result, for networks with many clusters, the probability of intercluster connections p_l required for achieving synchronization decreases as $1/M$. Note that $n^2(M-1)p_l \approx n^2 M p_l$ is the average number of intercluster links per cluster. This means, insofar as the average number of intercluster links per cluster is larger than certain critical value (depending on the dynamics), the network is always synchronizable, regardless of the number of clusters (the network size). This result is consistent with that in Ref. 43, which states that for random networks, one can have chaotic synchronization for any arbitrarily large network size, if the average degree is larger than some threshold.

The above analysis can be extended to more general clustered networks, i.e., those with different cluster sizes or heterogeneous degree distributions in each cluster, by replacing n with n_I—the size of the Ith cluster—for each I, and using the degree distribution $P_I(k)$ of the Ith cluster in the summation over $1/k$. In this case, p_s and p_l can be regarded as effective parameters, and may vary for different clusters. A formula similar to Eq. (10) can be obtained, because even in such a case, the contribution of the second term in Eq. (9) to λ_2 is small. This justifies that the observed abnormal synchronization phenomenon is due to the clustered network structure, and does not depend on the details of the dynamics.

B. Type-II coupling

For type-II coupling, the coupling matrix is defined as follows: for any i ($1 \leq i \leq N$), $G_{ii}=k_i$, $G_{ij}=-1$ if there is a link between nodes i and j, and $G_{ij}=0$ otherwise. The simulation results are shown in Fig. 7. In this case, we fix p_l =0.1 (so the number of intercluster connections is fixed), and examine the synchronizability of the system versus p_s. When p_s is small, there are frequent desynchronization bursts;[44,45] thus, the average fluctuation width $\langle\langle W\rangle_{T_0}\rangle_e$ is large and the system has a lower synchronization probability P_{syn}. As p_s increases, the system becomes more synchronizable and the intermittent desynchronization bursts become rare, and finally it stays synchronized in the whole time interval T_0 (about p_s=0.1). As p_s is increased further passing through a

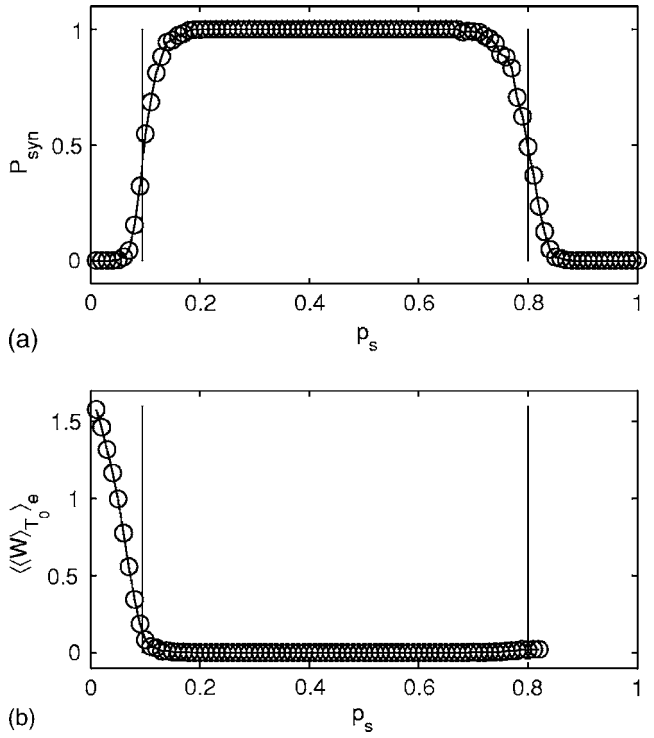

FIG. 7. Properties of the coupled Rössler system for type-II coupling. (a) The synchronization probability P_{syn} vs the intracluster connectivity probability p_s. (b) Ensemble averaged and time averaged fluctuation width $\langle\langle W\rangle_{T_0}\rangle_e$, where $p_l=0.1$, $T_0=20\,000$, $\delta=0.001$, $\epsilon=0.083$, $N=100$, and $M=2$. Vertical lines indicate the positions of the synchronization boundaries obtained from Eqs. (6) and (7), where the eigenvalues are calculated numerically. The absence of datapoints for large p_s in (b) means the system variables diverge. Each datapoint is the result of averaging over 1000 network realizations. The data for this figure were obtained with ten Pentium®-IV 2.80 GHz CPUs for about two weeks.

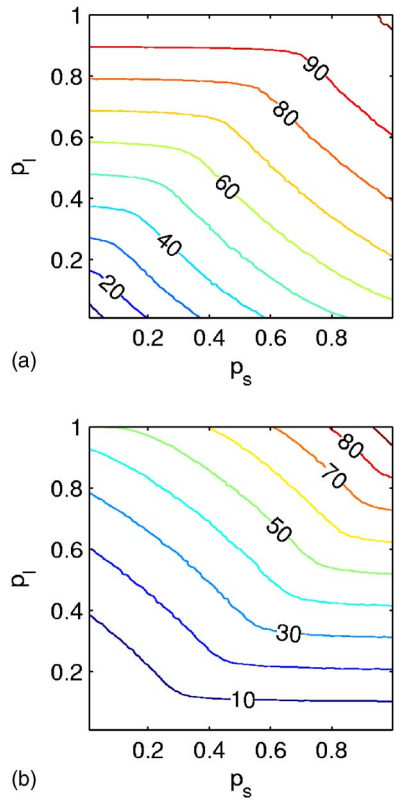

FIG. 8. (Color online) Contour plots of λ_N (a) and λ_2 (b) in the (p_l, p_s) space for type-II coupling, $N=100$ and $M=2$. Each datapoint is averaged over 100 realizations.

stable range $(0.1,0.8)$, the system becomes unstable. For even larger values of p_s, the system diverges for almost every network realization tested, which accounts for a small synchronization probability P_{syn}. The vertical lines in Fig. 7 show the positions of the synchronization boundaries obtained from Eqs. (6) and (7). It can be seen that the theory agrees well with the numerical simulations. The eigenvalues have been obtained numerically, and contour plots of λ_N and λ_2 in the network parameter space (p_l, p_s) are shown in Fig. 8. Therefore, under the stability boundary conditions Eqs. (6) and (7), the phenomenon that the synchronizability is deteriorated and destroyed in the presence of the mismatch in the numbers of intercluster and intracluster links for type-II coupling is also originated from the clustered structure and does not depend on the details of dynamical oscillators.

For type-II coupling, both λ_N and λ_2 will affect the synchronizable region, therefore we shall provide a theoretical approach for λ_N and λ_2 in terms of p_s and p_l for the case of $p_l \ll p_s$. For $p_l \ll p_s$, the largest eigenvalue of the system λ_N is on the same order of magnitude as the largest eigenvalue of one cluster λ_n; thus, it is reasonable to write $\lambda_N=\lambda_n+\delta$, where δ depends on p_l. Let us first consider λ_n. Since each cluster is a random network with size n and connecting probability p_s, λ_n is the largest eigenvalue of the coupling matrix of this random subnetwork $\mathbf{G_n}$. $\mathbf{G_n}$ can be decomposed as $\mathbf{G_n}=\mathbf{D_n}-\mathbf{A_n}$, where $\mathbf{D_n}$ is a diagonal matrix and $(D_n)_{ii}=k_i$, and $\mathbf{A_n}$ is the adjacency matrix of the random subnetwork defined as $(A_n)_{ij}=1$ if there is a link between node i and node j and 0 otherwise. It is known that the largest eigenvalue of $\mathbf{A_n}$ approaches np_s for large n, and the spectra density of the other eigenvalues satisfies a semicircle law:[47–50]

$$\rho(\lambda)=\begin{cases}(2\pi\sigma^2)^{-1}\sqrt{4\sigma^2-\lambda^2}, & \text{if } |\lambda|<2\sigma,\\ 0, & \text{otherwise},\end{cases}$$

where $\sigma=\sqrt{np_s(1-p_s)}$. Thus, the eigenvalues of $-\mathbf{A_n}$ have a minimum value of $-np_s$ and the others are approximately distributed in $(-2\sigma,2\sigma)$. Since the degree distribution of the random network is binomial with mean value of np_s and standard variation $\sigma_k=\sigma=\sqrt{np_s(1-p_s)}$, which is much smaller than the mean value np_s, $\mathbf{D_n}$ can be approximated as $\mathbf{D_n}\approx np_s\mathbf{I_n}$, where $\mathbf{I_n}$ is the identity matrix of order n. Adding $\mathbf{D_n}$ to $-\mathbf{A_n}$ only shifts all the eigenvalues of $-\mathbf{A_n}$ by the amount np_s, and moves the minimum eigenvalue of $-\mathbf{A_n}$ to 0, which is λ_1 of $\mathbf{G_n}$. Therefore, the largest eigenvalue of $\mathbf{G_n}$ is

$$\lambda_n(p_s)=np_s+2\sigma=np_s+2\sqrt{np_s(1-p_s)}. \tag{12}$$

To assess δ, note that when p_l is small, δ approximately depends on p_l only; i.e., $\partial\delta/\partial p_l \gg \partial\delta/\partial p_s$. Thus, $\delta(p_l,p_s)\approx\delta(p_l)$, which can be estimated at the point $p_s=p_l$:

$$\delta(p_l)=\lambda_N(p_l,p_l)-\lambda_n(p_l).$$

For $p_s=p_l$, the whole system is a homogeneous random network with connecting probability p_l; thus, the largest eigen-

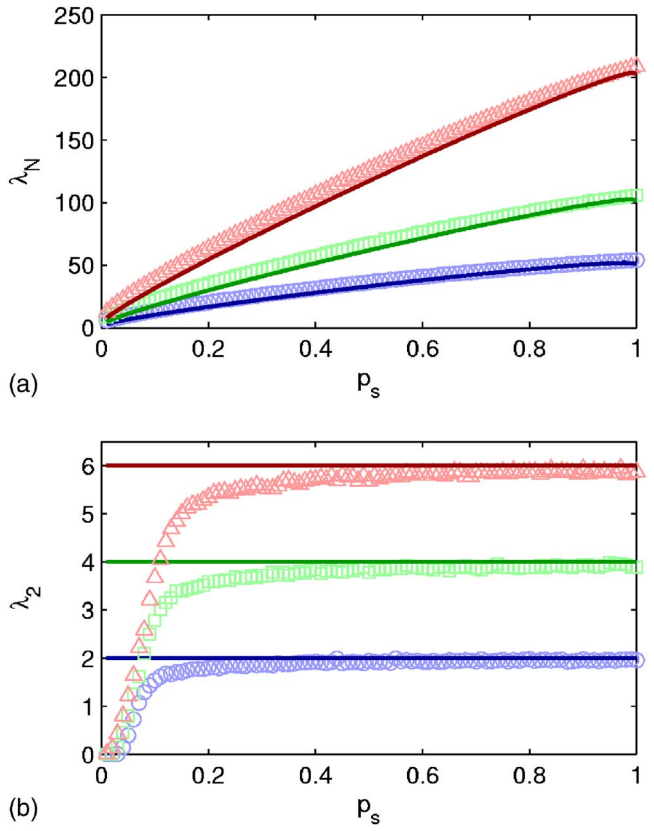

FIG. 9. (Color online) For type-II coupling, (a) the largest eigenvalue λ_N vs p_s for p_l=0.01 and N=100, 200, 400 from bottom to top, where M=2. Symbols are from direct numerical simulation, curves are from Eq. (13). (b) The smallest nontrivial eigenvalue λ_2 vs p_s for N=200, M=2, and p_l =0.01, 0.02, 0.03 from bottom to top. Symbols are from direct numerical simulation, the solid lines are from Eq. (14). Each datapoint is averaged over 100 realizations.

value can be obtained from Eq. (12): $\lambda_N(p_l,p_l)=Np_l+2\sqrt{Np_l(1-p_l)}$. We have

$$\delta(p_l)=(N-n)p_l+2(\sqrt{N}-\sqrt{n})\sqrt{p_l(1-p_l)},$$

and the largest eigenvalue of the random clustered network can be expressed as

$$\begin{aligned}\lambda_N(p_l,p_s)&=\lambda_n(p_s)+\delta(p_l)\\&=np_s+(N-n)p_l+2\sqrt{np_s(1-p_s)}\\&\quad+2(\sqrt{N}-\sqrt{n})\sqrt{p_l(1-p_l)}.\end{aligned}\tag{13}$$

Figure 9(a) shows the simulation results (symbols) of λ_N for different cases. The curves are from Eq. (13). It can be seen that the two fit well. Note that Eq. (13) is valid only for $p_l \ll p_s$. For $p_l > p_s$, the clustered structure vanishes and the decomposition of λ_N into λ_n is invalid.

We now turn our attention to λ_2. The corresponding eigenvector has a similar structure for type-II coupling as that for type-I coupling (see Fig. 5), therefore we have the same equation as Eq. (8). The coupling matrix is different from that of type-I coupling. In particular, $G_{ii}=k_i$, and if i and j belong to the same cluster, G_{ij} equals -1 with probability p_s and 0 with probability $1-p_s$, while if i and j belong to different clusters, G_{ij} equals -1 with probability p_l and 0 with probability $1-p_l$. We can thus write λ_2 as

$$\lambda_2=\sum_{i=1}^{N}e_{2i}\{-np_l\tilde{e}_1-np_l\tilde{e}_2+\cdots+k_i\tilde{e}_I-np_s\tilde{e}_I+\cdots-np_l\tilde{e}_M\},$$

where $\tilde{e}_I$ is the value corresponding to the cluster that contains node i. Noting that $k_i\approx k=np_s+(N-n)p_l$, under similar manipulations to those for type-I coupling, we have

$$\begin{aligned}\lambda_2&=\sum_{i=1}^{N}e_{2i}\left\{(N-n)p_l\tilde{e}_I-np_l\sum_{J\neq I}^{M}\tilde{e}_J\right\}\\&=\sum_{i=1}^{N}e_{2i}\left\{Np_l\tilde{e}_I-np_l\sum_{J=1}^{M}\tilde{e}_J\right\}\\&\approx\sum_{I=1}^{M}n\tilde{e}_I\left\{Np_l\tilde{e}_I-np_l\sum_{J=1}^{M}\tilde{e}_J\right\}\\&=Np_l\sum_{I=1}^{M}n\tilde{e}_I^2-\left(n\sum_{J=1}^{M}\tilde{e}_J\right)^2p_l.\end{aligned}$$

Note that $\Sigma_{I=1}^{M}n\tilde{e}_I^2\approx\Sigma_{i=1}^{N}e_{2i}^2=1$, and $n\Sigma_{J=1}^{M}\tilde{e}_J=\Sigma_{i=1}^{N}e_{2i}=0$ (**G** is symmetric for type-II coupling), finally, we have

$$\lambda_2\approx Np_l.\tag{14}$$

Figure 9(b) shows the dependence of λ_2 on p_s. The theory [Eq. (14), curves] agrees well with the numerical simulations (symbols). The analytical results about λ_N and λ_2 [Eqs. (13) and (14)] explain the patterns in Fig. 8 for the $p_l<p_s$ region. Since λ_N increases with p_s, for large p_s, λ_N could be too large, leading to an instability in the corresponding eigenmode of the system. This explains that too many intracluster links can depress the synchronizability of the system.

IV. DISCUSSION

In conclusion, we have presented theory and numerical evidence that optimal synchronization of continuous-time oscillator clustered networks can be achieved by matching the probabilities of intercluster and intracluster links. That is, at a global level, the network has the strongest synchronizability when these probabilities are approximately equal. Overwhelmingly strong intracluster connection can counterintuitively weaken the network synchronizability. This can be better understood by the following considerations. Network synchronizability is usually characterized by the spread of the nontrivial eigenvalues. What our analytical formulae suggest is that spread becomes minimal when the two probabilities are approximately matched. For instance, when the intercluster linking probability p_l is fixed, increasing the intracluster connection probability p_s could result in desynchronization. On the other hand, for realistic clustered networks, p_l is always smaller than p_s, and is usually much smaller. Our analysis indicates that, insofar as the network is clustered ($p_s>p_l$), a larger p_l will lead to better synchronizability. To give another example, consider a particular set of (p_l, p_s) values for which the network cannot be synchronized. Then, increasing p_l while decreasing p_s (so as to keep the average degree fixed) can lead to synchronization (Figs. 4 and 8). While our theory gives a general picture for the net-

work synchronizability in the two-dimensional parameter plane (p_l, p_s), the optimal cases where the two probabilities match approximately do not seem to occur in realistic situations, where p_l is usually much smaller than p_s.

While our network model is somewhat idealized, we have argued that similar phenomena should persist in more general clustered networks. In real biological or technological systems with a clustered structure, if global synchronization is the best performance of the system, special attention needs to be paid to distinguishing the interconnections and intraconnections as in this case, a proper distribution of the links is more efficient than adding links blindly. For biological networks, such as the metabolic network and the protein-protein interaction network, certain nodes may have many more links than the others, forming a hierarchical clustered structure.[29] This indicates a power-law distribution of the degree k: $P(k) \sim k^{-\gamma}$. Therefore, it is interesting to study clustered scale-free networks, networks where each cluster contains a scale-free subnetwork. We have studied the synchronizability of such clustered networks. In particular, for each cluster, the subnetwork was generated via the preferential attachment rule.[5] Initially, there is a fully connected small subset of size m_0, then a new node is added with m links, and the probability that a previous node i is connected to this new node is proportional to its current degree k_i. New nodes are continuously added until a prescribed network size n is reached. In our simulation, we take $m_0=2m+1$, so that the average degree of this network is $2m$. M such scale-free subnetworks are generated. We then connect each pair of nodes in different clusters with probability p_l. For this model, p_l controls the number of intercluster links, and m controls the number of intracluster links. We have carried out numerical simulations, and have found that the patterns for the eigenvalues λ_N and λ_2 are essentially the same as that for the clustered network where each cluster contains a random subnetwork (Figs. 4 and 8). In fact, we have compared the simulation results to Eq. (10) for the type-I coupling, where we took $p_s=2m/n$. The mean field theory Eq. (10) fits reasonably well with the simulation results. This indicates that optimization of synchronization by matching different types of links is a general rule.

The general observation is that the synchronizability of the clustered networks is mainly determined by the underlying clustered structure. Insofar as there is a clustered structure, details such as how nodes within a cluster connect to each other, what kind of dynamics are carried by the network and what the parameters are, do not appear to have a significant influence on the synchronization in the coupled oscillator networks supported by the clustered backbone. A practical usage is that, even if the details about the dynamics of a realistic system are not available, insofar as the underlying network has a clustered structure, we can expect similar synchronization behaviors as presented in this paper.

An interesting issue about the synchronization dynamics on a clustered network is how it desynchronizes. As discussed in Refs. 44 and 45, when desynchronization occurs, the deviation from the synchronization state, $x_i-\langle x_i\rangle$, will have the same form as the unstable eigenmodes (eigenvectors). As a result, if the desynchronization is caused by λ_2's being too small [violation of condition (6)], the desynchronized dynamics will have a clustered structure, due to a clustered structure in the corresponding eigenvector $\mathbf{e}_2$: nodes within a cluster have approximately the same dynamical variables, while they can be quite different among clusters. That is, desynchronization occurs among clusters. However, if the desynchronization is caused by λ_N's being too large [violation of condition (7)], the deviation $x_i-\langle x_i\rangle$ will not have a clustered structure, since $\mathbf{e}_N$ typically does not exhibit any clustered features. In this case, desynchronization occurs both among and within clusters.

The clustered topology has also been identified in technological networks such as computer networks and certain electronic circuit networks.[2,3,51] For a computer network, the main functions include executing sophisticated codes to carry out extensive computations. Suppose a large-scale, parallel computational task is to be accomplished by the network, for which synchronous timing is of paramount importance. Our result can provide useful clues as to how to design the network to achieve the best possible synchronization and consequently optimal computational efficiency.

ACKNOWLEDGMENTS

We thank Dr. Kwangho Park for valuable discussions. This work is supported by an ASU-UA Collaborative Program on Biomedical Research, by NSF under Grant No. ITR-0312131 and by AFOSR under Grant Nos. F49620-01-01-0317 and FA9550-06-1-0024.

[1] L. C. Jia, M. Sano, P.-Y. Lai, and C. K. Chan, Phys. Rev. Lett. **93**, 088101 (2004).
[2] A. Vázquez, R. Pastor-Satorras, and A. Vespignani, Phys. Rev. E **65**, 066130 (2002).
[3] K. A. Eriksen, I. Simonsen, S. Maslov, and K. Sneppen, Phys. Rev. Lett. **90**, 148701 (2003).
[4] D. J. Watts and S. H. Strogatz, Nature (London) **393**, 440 (1998).
[5] A.-L. Barabási and R. Albert, Science **286**, 509 (1999).
[6] Y. Ho, A. Gruhler, A. Heilbut, G. D. Bader, L. Moore, S. L. Adams, A. Millar, P. Taylor, K. Bennett, K. Boutilier, L. Yang, C. Wolting, I. Donaldson, S. Schandorff, J. Shewnarane, M. Vo, J. Taggart, M. Goudreault, B. Muskat, C. Alfarano, D. Dewar, Z. Lin, K. Michalickova, A. R. Willems, H. Sassi, P. A. Nielsen, K. J. Rasmussen, J. R. Andersen, L. E. Johansen, L. H. Hansen, H. Jespersen, A. Podtelejnikov, E. Nielsen, J. Crawford, V. Poulsen, B. D. Sørensen, J. Matthiesen, R. C. Hendrickson, F. Gleeson, T. Pawson, M. F. Moran, D. Durocher, M. Mann, C. W. Hogue, D. Figeys, and M. Tyers, Nature (London) **415**, 180 (2002).
[7] V. Spirin and L. A. Mirny, Proc. Natl. Acad. Sci. U.S.A. **100**, 12123 (2003).
[8] G. Palla, I. Derényi, I. Farkas, and T. Vicsek, Nature (London) **435**, 814 (2005).
[9] E. Ravasz, A. L. Somera, D. A. Mongru, Z. Oltvai, and A.-L. Barabási, Science **297**, 1551 (2002).
[10] K. Park, Y.-C. Lai, S. Gupte, and J.-W. Kim, Chaos **16**, 015105 (2006).
[11] L. Huang, K. Park, Y.-C. Lai, L. Yang, and K. Yang, Phys. Rev. Lett. **97**, 164101 (2006).
[12] L. F. Lago-Fernandez, R. Huerta, F. Corbacho, and J. A. Siguenza, Phys. Rev. Lett. **84**, 2758 (2000).
[13] P. M. Gade and C.-K. Hu, Phys. Rev. E **62**, 6409 (2000).
[14] M. Barahona and L. M. Pecora, Phys. Rev. Lett. **89**, 054101 (2002).
[15] X. F. Wang and G. Chen, Int. J. Bifurcation Chaos Appl. Sci. Eng. **12**, 187 (2002).
[16] X. F. Wang and G. Chen, IEEE Trans. Circuits Syst., I: Fundam. Theory Appl. **49**, 54 (2002).
[17] H. Hong, M. Y. Choi, and B. J. Kim, Phys. Rev. E **65**, 026139 (2002).

[18]S. Jalan and R. E. Amritkar, Phys. Rev. Lett. **90**, 014101 (2003).
[19]T. Nishikawa, A. E. Motter, Y.-C. Lai, and F. C. Hoppensteadt, Phys. Rev. Lett. **91**, 014101 (2003).
[20]A. E. Motter, C. Zhou, and J. Kurths, Europhys. Lett. **69**, 334 (2005).
[21]A. E. Motter, C. Zhou, and J. Kurths, Phys. Rev. E **71**, 016116 (2005).
[22]C. Zhou, A. E. Motter, and J. Kurths, Phys. Rev. Lett. **96**, 034101 (2006).
[23]M. Chavez, D.-U. Hwang, A. Amann, H. G. E. Hentschel, and S. Boccaletti, Phys. Rev. Lett. **94**, 218701 (2005).
[24]F. M. Atay, T. Bıyıkoğlu, and J. Jost, IEEE Trans. Circuits Syst., I: Regul. Pap. **53**, 92 (2006).
[25]T. Ideker, Adv. Exp. Med. Biol. **547**, 21 (2004).
[26]Y. Xia, H. Yu, R. Jansen, M. Seringhaus, S. Baxter, D. Greenbaum, H. Zhao, and M. Gerstein, Annu. Rev. Biochem. **73**, 1051 (2004).
[27]M. Lappe and L. Holm, Nat. Biotechnol. **22**, 98 (2004).
[28]B. P. Kelley, R. Sharan, R. M. Karp, T. Sittler, D. E. Root, B. R. Stockwell, and T. Ideker, Proc. Natl. Acad. Sci. U.S.A. **100**, 11394 (2003).
[29]A.-L. Barabási and Z. N. Oltvai, Nat. Rev. Genet. **5**, 101 (2004).
[30]R. Albert and A.-L. Barabási, Rev. Mod. Phys. **74**, 47 (2002).
[31]M. E. J. Newman, SIAM Rev. **45**, 167 (2003).
[32]S. N. Dorogovtsev and J. F. F. Mendes, *Evolution of Networks* (Oxford University Press, Oxford, 2003).
[33]R. Pastor-Satorras and A. Vespignani, *Evolution and Structure of the Internet* (Cambridge University Press, Cambridge, 2004).
[34]D. J. Watts, P. S. Dodds, and M. E. J. Newman, Science **296**, 1302 (2002).
[35]A. E. Motter, T. Nishikawa, and Y.-C. Lai, Phys. Rev. E **68**, 036105 (2003).
[36]E. Oh, K. Rho, H. Hong, and B. Kahng, Phys. Rev. E **72**, 047101 (2005).
[37]S. Strogatz, *Sync: The Emerging Science of Spontaneous Order* (Hyperion, New York, 2003).
[38]J. B. Buck and E. Buck, Science **159**, 1319 (1968).
[39]C. S. Peskin, in *Physiology* (Courant Institute of Mathematical Sciences, New York, 1975).
[40]A. Sherman and J. Rinzel, Biophys. J. **59**, 547 (1991).
[41]J. Dye, J. Comp. Physiol., A **168**, 521 (1991).
[42]L. M. Pecora and T. L. Carroll, Phys. Rev. Lett. **80**, 2109 (1998).
[43]J. Jost and M. P. Joy, Phys. Rev. E **65**, 016201 (2002).
[44]J. G. Restrepo, E. Ott, and B. R. Hunt, Phys. Rev. Lett. **93**, 114101 (2004).
[45]J. G. Restrepo, E. Ott, and B. R. Hunt, Phys. Rev. E **69**, 066215 (2004).
[46]B. Gong, L. Yang, and K. Yang, Phys. Rev. E **72**, 037101 (2005).
[47]E. P. Wigner, Ann. Math. **62**, 548 (1955).
[48]E. P. Wigner, Ann. Math. **65**, 203 (1957).
[49]M. L. Mehta, *Random Matrices*, 2nd ed. (Academic, New York, 1991).
[50]I. J. Farkas, I. Derényi, A.-L. Barabási, and T. Vicsek, Phys. Rev. E **64**, 026704 (2001).
[51]R. Milo, S. Shen-Orr, S. Itzkovitz, N. Kashtan, D. Chklovskii, and U. Alon, Science **298**, 824 (2002).